

DOI: 10.17516/1997-1397-2022-15-4-450-458

УДК 541.122: 538.214

ESR and ^{57}Fe Mössbauer Spectroscopy Study of Fe-doped $\text{SrBi}_2\text{Nb}_2\text{O}_9$

Vladimir P. Lyutoev*

Andrey Yu. Lysiuk[†]

Institute of Geology of the Komi Science Center UB RAS
Syktyvkar, Russian Federation

Larisa O. Karlova[‡]

JSC "Komi Thermal Company"
Syktyvkar, Russian Federation

Dmitriy S. Beznosikov[§]

Federal State Unitary Enterprise "General Radio Frequency Centre"
Northwestern Federal District Branch
Syktyvkar, Russian Federation

Nadezhda A. Zhuk[¶]

Pitirim Sorokin Syktyvkar State University
Syktyvkar, Russian Federation

Received 10.09.2021, received in revised form 13.02.2022, accepted 20.04.2022

Abstract. Solid solutions of $\text{Bi}_2\text{SrNb}_{2-2x}\text{Fe}_{2x}\text{O}_{9-\delta}$ have been obtained by solid-phase synthesis. The electronic state and nature of the local environment of iron atoms in the $\text{SrBi}_2\text{Nb}_2\text{O}_9$ matrix with a layered perovskite-like structure were studied by ESR and Mössbauer spectroscopy. In the ESR spectra of samples of $\text{Bi}_2\text{SrNb}_{2-2x}\text{Fe}_{2x}\text{O}_{9-\delta}$ ($x \leq 0.04$) solid solutions an intensive asymmetric line in the low-field region with the main feature at $g = 4.27$, weakly pronounced peak $g = 6.15$ and shoulder $g \sim 9$, and also an intensive broad ($\Delta B_{pp} \sim 50\text{--}150$ mT) band centered around $g \sim 2.0$ is present. The Mössbauer spectrum of the compound $\text{Bi}_2\text{SrNb}_{2-2x}\text{Fe}_{2x}\text{O}_{9-\delta}$ is represented by an asymmetric doublet with isomer shift (IS) ~ 0.3 , and quadrupole splitting (QS) ~ 0.5 mm/s. The shape of the doublet is reproduced by the superposition of two doublets with small and high IS and QS values. About 85% of the spectral area of the paramagnetic part of the spectrum is represented by the doublet $\text{Fe}^{3+}(1)$ with $\text{IS} = 0.31 \pm 0.04$, $\text{QS} = 0.45 \pm 0.04$ mm/s correlated with Fe^{3+} ions in regular axial positions. The remaining part is represented by the doublet $\text{Fe}^{3+}(2)$ with $\text{IS} = 0.5 \pm 0.1$, $\text{QS} = 0.7 \pm 0.2$ mm/s from the Fe^{3+} ions in defect environment.

Keywords: Aurivillius phases, iron, ESR, Mössbauer spectroscopy.

Citation: V.P. Lyutoev, A.Yu. Lysiuk, L.O. Karlova, D.S. Beznosikov, N.A. Zhuk, ESR and ^{57}Fe Mössbauer Spectroscopy Study of Fe-doped $\text{SrBi}_2\text{Nb}_2\text{O}_9$, J. Sib. Fed. Univ. Math. Phys., 2022, 15(4), 450–458. DOI: 10.17516/1997-1397-2022-15-4-450-458.

*vlutoev@geo.komisc.ru <https://orcid.org/0000-0003-0231-302X>

[†]andra227@yandex.ru <https://orcid.org/0000-0003-3868-4586>

[‡]larisa.karlova@yandex.ru

[§]svn71p3@gmail.com

[¶]nzhuck@mail.ru <https://orcid.org/0000-0002-9907-0898>

© Siberian Federal University. All rights reserved

The unremitting interest of scientists in Aurivillius phases is due to the manifestation of a wide range of practically useful properties [1–3]. They have high Curie temperatures, low degradation rates of residual polarization and piezoelectric properties when exposed to unipolar electric fields, and high dielectric permittivity, which necessitates their use as components of composite film systems for long term information storage (FRAM) processing devices, as well as the manufacture of piezo- and pyroelectric transducers based on them [4, 5]. In the crystal structure of Aurivillius phases described by the general formula $A_{m-1}\text{Bi}_2\text{B}_m\text{O}_{3m+3}$, fluorite-like $[\text{Bi}_2\text{O}_2]^{2+}$ and perovskite-like $[\text{A}_{m-1}\text{B}_m\text{O}_{3m+1}]^{2-}$ layers alternate, where cationic A-positions with cuboctahedral environment are occupied by ions of large radius (Na^+ , K^+ , Ca^{2+} , Sr^{2+} , Ba^{2+} , Pb^{2+} , Bi^{3+} , La^{3+}), and in octahedral positions B the highly charged small-radius cations (Cr^{3+} , Ga^{3+} , Fe^{3+} , Co^{3+} , Ti^{4+} , Mn^{4+} , Nb^{5+} , Ta^{5+} , Mo^{6+} , W^{6+}) are located [6–13]. The m parameter corresponds to the number of $[\text{A}_{m-1}\text{B}_m\text{O}_{3m+1}]^{2-}$ layers in the perovskite-like block. In the crystal structure of bismuth-strontium niobate $\text{Bi}_2\text{SrNb}_2\text{O}_9$ (sp. gr. $A2_{1am}$, $a = 0.55189(3)$, $b = 0.55154(3)$ and $c = 2.51124(9)$ nm) bismuth-oxygen layers alternate with perovskite-like blocks of two niobium-oxygen octahedral thickness. The size discrepancy between the cuboctahedral cavities of the perovskite-like blocks and the strontium atoms leads to geometrical distortions in the structure which manifest in asymmetry and angular inclination of the niobium-oxygen octahedrons [9, 14, 15], and the partial replacement of Bi^{3+} ions in fluorite-like layers by Sr^{2+} ions leads to a blurring of the phase transition and a relaxation character of dielectric polarization ($T_c = 420\text{--}440$ °C) [16]. As shown in [17], the Curie temperature can naturally increase with the Fe^{3+} ions concentration in $\text{SrBi}_2\text{Nb}_{2-x}\text{Fe}_x\text{O}_9$ ceramics and for $x=0$. it increases up to 524 °C. It is shown that the Fe-doped $\text{SrBi}_2\text{Nb}_2\text{O}_9$ phase-pure ceramics are formed in wide concentration interval $x \leq 0.4$ and exhibit the properties of magnetoelectric multiferroics. The occurrence of antiferromagnetic properties of the samples is explained by the superexchange interaction ($\text{Fe}^{3+}\text{-O-Fe}^{3+}$). Previous studies of magnetic dilution and ESR of iron-containing bismuth niobate solid solutions $\text{Bi}_2\text{BaNb}_2\text{O}_9$, $\text{Bi}_2\text{SrNb}_2\text{O}_9$ ($m = 2$) and $\text{Bi}_5\text{Nb}_3\text{O}_{15}$ ($m = 1.5$) showed [18–23] that iron Fe^{3+} ions preferentially replace the octahedral positions of Nb^{5+} ions and tend to aggregate to form high-nucleus antiferromagnetic clusters. This work presents for the first time the results of the study of the electronic state and local environment of iron atoms in solid solutions $\text{Bi}_2\text{SrNb}_{2-2x}\text{Fe}_{2x}\text{O}_{9-\delta}$ by ESR and Mössbauer spectroscopy.

1. Materials and methods

The samples of the bismuth barium niobate solid solutions were synthesized by the standard ceramic method from the "special purity grade" bismuth (III), niobium (V) and iron (III) oxides by the staged calcination at 650, 850, 950 and 1050 °C. The phase composition of the samples was controlled by X-ray phase analysis (Shimadzu 6000, $\text{CuK}\alpha$ -radiation). Microstructure and local chemical composition of the samples were studied by electron scanning microscopy (Tescan MIRA 3LMN, INCA Energy 450). The unit cell parameters of the solid solutions were calculated using the CSD software package [24]. The ESR spectra were recorded with an X-band radiospectrometer SE/X-2547 (RadioPAN) in the Shared Services Center "Geonauka" at the Institute of Geology FRC Komi SC UB RAS. The spectra recording was done with a rectangular resonator (RX102, mode TE 102) at room temperature as a first-order derivative at high-frequency modulation 100 MHz with amplitude 0.25 mT and microwave field strength 35 mW. A sample powder (approx 100 mg) was put into a quartz tube with external diameter of 4 mm. To calibrate the amplification of the equipment, an ESR signal from a miniature reference sample (anthracite,

singlet line with $g = 2.003$ and peak to peak width $\Delta B_{pp} = 0.5$ mT) was used. For each sample the spectrum was recorded within the range of magnetic fields 0–700 mT, and the lines of the reference standard with scanning 5 mT were recorded separately. The samples spectra were adjusted to equal values of the reference standard intensity and normalized on the equal weight of the sample. The ^{57}Fe Mössbauer spectra were obtained on an MS-1104 Em spectrometer at the rates of $-11 - +11$ mm/s at room temperature. The 6×10^8 Bq ^{57}Co in chrome matrix (Ritverc GmbH, St. Petersburg) was used at RT. To eliminate the texturing effects in the spectra, the samples were prepared in the form of finely ground powder. The duration of spectrum accumulation was about 260 hours. The isomeric shift was determined relative to $\alpha\text{-Fe}$. The spectra were processed using the standard software of a spectrometer "Univem".

2. Results and discussion

The samples of composition $\text{Bi}_2\text{SrNb}_{2-2x}\text{Fe}_{2x}\text{O}_{9-\delta}$ ($x \leq 0.08$) were obtained by solid-phase synthesis. It is found that grains of all samples are densely packed and form almost porous microstructure (Fig. 1). The samples contain chaotically oriented, mainly lamellar anisotropic grains that is also typical for ceramics of Aurivillius phase [25, 26].

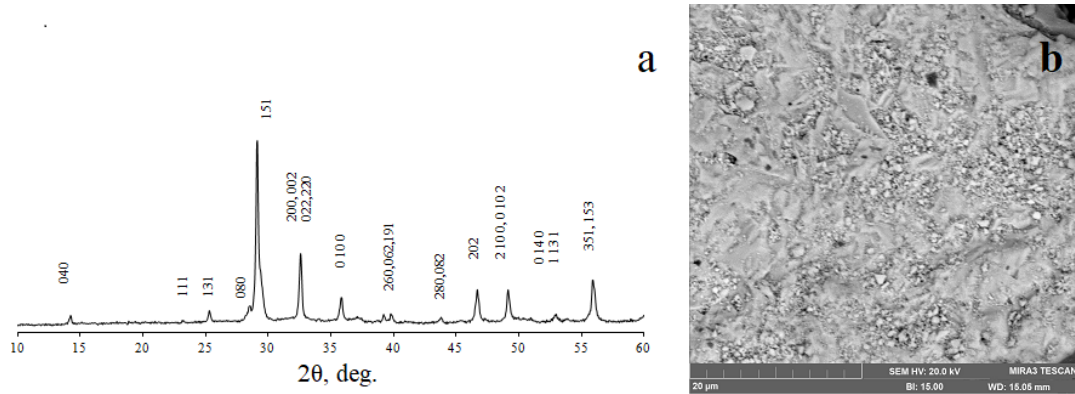


Fig. 1. X-ray diffraction (a) and microphotograph (b) of the $\text{Bi}_2\text{SrNb}_{1.90}\text{Fe}_{0.10}\text{O}_{9-\delta}$ in the mode of elastically reflected electrons

According to the X-ray phase analysis the iron-containing solid solutions are formed in the limited concentration interval $x \leq 0.05$. X-ray examination of the obtained solid solutions showed that their crystal structure corresponds to the structure of $\text{Bi}_2\text{SrNb}_2\text{O}_9$. With increasing iron content in solid solutions, parameters a and b decrease, and c increases: $a = 0.55045$ nm, $b = 0.55066$ nm, $c = 2.5054$ nm ($x = 0.003$) to $a = 0.55017$ nm, $b = 0.55037$ nm, $c = 2.5072$ nm ($x = 0.05$). Apparently, the unit cell parameter c slightly increases due to the isomorphic replacement of octahedral Nb^{5+} cations in perovskite-like layers by Fe^{3+} ions with a slightly larger radii: $R(\text{VI}\text{Nb}^{5+}) = 0.064$; $R(\text{VI}\text{Fe}^{3+}) = 0.0645$ nm [27]. This assumption does not contradict our ESR studies.

In the ESR spectra of solid solution samples of $\text{Bi}_2\text{SrNb}_{2-2x}\text{Fe}_{2x}\text{O}_{9-\delta}$ ($x = 0.005, 0.02, 0.04$) there is an intensive asymmetric line in the low-field region with the main feature at $g = 4.27$, weakly pronounced peak $g = 6.15$ and shoulder $g \sim 9$, and also an intensive broad ($\Delta B_{pp} \sim 50\text{--}150$ mT) band centered around $g \sim 2.0$ (Fig. 2). The origin of $g = 4.27$ component is associated with structurally isolated Fe^{3+} ions in a strong octahedral crystal field with

$D > 10$ GHz, and a maximum degree of rhombic distortion $E/D \sim 1/3$ [21]. At that the effective g-factor of the transition line between the Kramers doublet $\pm 3/2$ levels becomes isotropic and equals 4.27. In amorphous and polycrystalline materials, such as ceramics, the isotropic 4.27 line is not subject to orientational broadening and dominates over the lines of other transitions with anisotropic effective g-factors. The broad prevalence of line 4.27 may be related to distributed values of crystal field parameters in low-ordered matrices. Due to peculiarities of orientation broadening of lines in polycrystalline and amorphous material in the ESR spectrum a small fraction of D and E distribution in the region of $D > 10$ GHz, $E/D \sim 1/3$ are mainly observed. Low-intensity lines $g = 6.15, 9$ probably represent part of the spectrum from isolated Fe^{3+} ions in the axial crystalline field ($E = 0$). Relatively low-intensity signal in the region $g \sim 2.0$ in the spectrum of the sample with $x = 0.005$ is also a component of the spectrum from the isolated axial Fe^{3+} ions. At high values of x the band $g \sim 2.0$ is strongly broadened and belongs mainly to clusters of iron ions.

The axial ($E \sim 0$) ESR spectrum of Fe^{3+} in the compound $\text{Bi}_2\text{SrNb}_{2-2x}\text{Fe}_{2x}\text{O}_{9-\delta}$ can appear at isovalent substitution of $\text{Fe}^{3+} \rightarrow \text{Bi}^{3+}$, which is unlikely because of the large difference of ionic radii. The axial spectrum can be also connected with regular iron positions by the scheme of heterovalent isomorphism $\text{Fe}^{3+}\text{O}_6 \rightarrow \text{Nb}^{5+}\text{O}_6 + \text{V}[\text{O}^{2-}]$. Compensation of excess negative charge is carried out by axial oxygen vacancy in the second coordination sphere. In defective crystal regions and in near-surface layers the Fe^{3+}O_6 complex undergoes strong rhombic distortion ($E \sim 1/3$), that gives rise to the 4.27 line in the ESR spectrum. The broad band $g \sim 2.0$ is associated with clusters of these iron ions. Fractions of axial, rhombically distorted and clustered Fe^{3+} positions cannot be estimated by the intensities of corresponding lines because of their concentration dependence is sharply nonlinear. Even with an insignificant fraction of Fe^{3+} in the ($E \sim 1/3$) position, the isotropic narrow line with $g = 4.27$ will dominate the ESR spectrum.

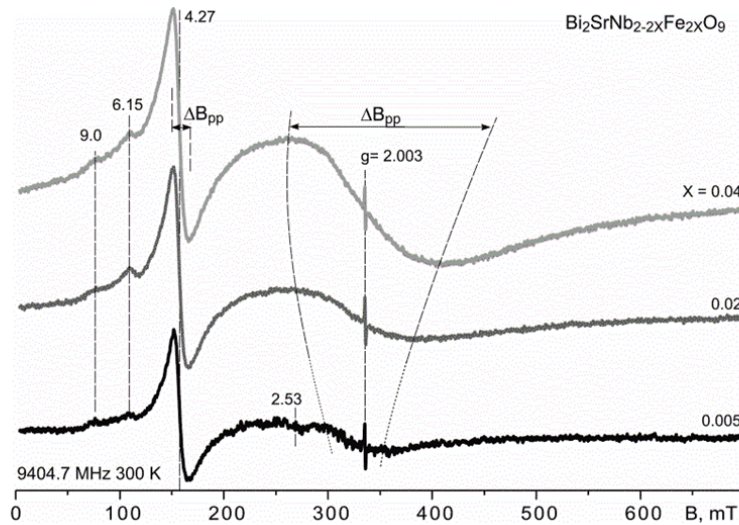


Fig. 2. ESR spectra of the samples of the $\text{Bi}_2\text{SrNb}_{2-2x}\text{Fe}_{2x}\text{O}_{9-\delta}$ solid solutions at various values of index x . Reference sample line with $g=2.003$

The iron atoms clustering was first suggested in [18, 19], a study of magnetic dilution in Fe-doped $\text{Bi}_2\text{SrNb}_2\text{O}_9$. It was found that in strongly diluted solid solution, iron ions are aggregated

in the form of clusters with antiferroic and ferromagnetic types of exchange. With increasing iron concentration, the proportion of aggregates with the antiferromagnetic type of exchange only increases. Even in strongly dilute solutions of $\text{Bi}_2\text{SrNb}_{2-2x}\text{Fe}_{2x}\text{O}_{9-\delta}$, iron atoms tendency to form exchange-bonded aggregates is caused by the considerable covalence of Fe-O bond and the predominance of antiferromagnetic exchange connected with the overlap ferric and oxygen atomic orbitals in clusters. It is shown that geometrical distortions of $\text{Bi}_2\text{SrNb}_2\text{O}_9$ structure have a significant influence on the nature and intensity of the exchange interaction between paramagnetic atoms in highly dilute iron-containing solid solutions. The presence of clusters with antiferro- and ferromagnetic type of exchange may indicate the presence of Fe^{3+} ions in crystal fields of different symmetry.

In order to investigate the character of the local environment of iron ions the Mössbauer spectroscopy was used. Mössbauer spectrum of $\text{Bi}_2\text{SrNb}_{2-2x}\text{Fe}_{2x}\text{O}_{9-\delta}$ compound was obtained at $x = 0.08$. But even at very long accumulation of spectrum (260 h) the achieved effect error was more than 15%. Fig. 3 shows the paramagnetic ($-3 - +3$ mm/s) part of the full spectrum ($-11 - +11$ mm/s). The paramagnetic part of the spectrum is represented by an asymmetric doublet with isomer shift (IS) ~ 0.3 and quadrupole splitting (QS) ~ 0.5 mm/s. Along its edges the features with IS ~ -0.6 and $+1.7$ mm/s are poorly distinguishable, which we attributed to the internal pair of sextet lines from the magnetically ordered iron oxide. These are the narrowest lines and less susceptible to sextet line broadening. In their spectral position they correspond to Fe_2O_3 hematite: IS ≈ 0.4 mm/s, QS ≈ -0.3 mm/s and superfine magnetic field at Fe nuclei 400 kOe [28]. It is possible, that these are rudiments of formation of the condensed iron oxide phase on iron (III) clusters observed by ESR at lower iron content in ceramics. This conclusion can contradict results of work [17], at that we deal with poorly resolved spectrum.

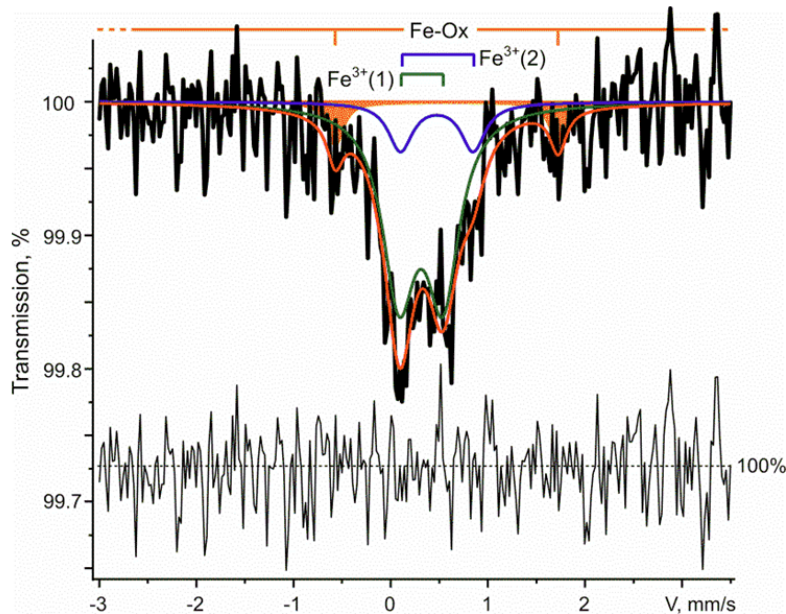


Fig. 3. ^{57}Fe Mössbauer spectra of the samples $\text{Bi}_2\text{SrNb}_{2-2x}\text{Fe}_{2x}\text{O}_{9-\delta}$ ($x = 0.08$) in the paramagnetic region. The fitted components: Fe-Ox — internal line of sextet of the magnetically ordered iron oxide; $\text{Fe}^{3+}(1,2)$ — paramagnetic doublets of the dissolved in the crystalline structure of ceramics Fe^{3+} ions

The asymmetry of the paramagnetic doublet $IS \sim 0.3$, $QS \sim 0.5$ mm/s is a consequence of its non-elementarity. Its shape is reproduced by the superposition of two doublets with small and high IS and QS values. About 85% of the spectral area of the paramagnetic part of the spectrum falls on the doublet $\text{Fe}^{3+}(1)$ with $IS = 0.31 \pm 0.04$, $QS = 0.45 \pm 0.04$ mm/s, the remaining part is represented by the doublet $\text{Fe}^{3+}(2)$ with $IS = 0.5 \pm 0.1$, $QS = 0.7 \pm 0.2$ mm/s. The first one, with a lower quadrupole splitting, is reasonable to associate with Fe^{3+} ions in regular axial positions $\text{Fe}^{3+}\text{O}_6 \rightarrow \text{Nb}^{5+}\text{O}_6 + \text{V}[\text{O}^{2-}]$, proposed in the analysis of ESR spectra. This is confirmed by Mössbauer studies of compounds in which Fe^{3+} ions have octahedral coordination [29–31]. For example, for the compound $\text{Bi}_2\text{FeNbO}_7$ the parameters of the Mössbauer spectrum for $^{57}\text{Fe}^{3+}$: $IS = 0.27$ mm/s, $QS = 0.41$ mm/s [29], in the iron-containing Aurivillius phase $\text{Bi}_5\text{FeTi}_3\text{O}_{15}$ octahedral Fe^{3+} ions appear in the spectrum with parameters $IS = 0.38$ mm/s, $QS = 0.60$ mm/s [30]. Then, the second doublet $\text{Fe}^{3+}(2)$ with large quadrupole splitting, refers to the Nb^{5+} substituted Fe^{3+} ions in the defect environment. The assumption that Fe^{3+} ions can substitute the Bi^{3+} ions positions is not supported by the spectrum parameters. As shown in [30, 31], the quadrupole splitting of such Fe^{3+} ions is higher or is near unity. As shown earlier [32, 33], Fe^{3+} ions are more prone to highly symmetric coordination and, due to the ionic radius and polarization properties, prefer the octahedral coordination of Nb^{5+} ions from the two alternative cationic positions. It can only be assumed that the Fe^{3+} ions associated with oxygen vacancies, characterized by low quadrupole splitting and representing about 85% of the total iron content in the niobate lattice, are in an aggregated state, while the other iron ions are predominantly in the monomeric state. The conclusion about the presence of the Fe^{3+} ions in oxygen environment of different geometries is supported by the results of magnetodilution studies in Fe-doped $\text{Bi}_2\text{SrNb}_2\text{O}_9$ ceramics [18, 19] under the assumption of clusters with antiferro- and ferromagnetic exchange type.

Conclusions

$\text{Bi}_2\text{SrNb}_{2-2x}\text{Fe}_{2x}\text{O}_{9-\delta}$ solid solutions in the limited concentration range were obtained by ceramic synthesis. The samples are characterized by a porous microstructure formed by chaotically arranged plate-shaped anisotropic grains. Results of ESR and Mössbauer spectroscopy reveal three forms of iron localization in ceramics: isolated Fe^{3+} ions in regular and defective octahedral positions of Nb^{5+} substitution and clusters of iron ions up to the formation of iron oxide phase. The major part of Fe^{3+} ions is located in regular octahedral positions of Nb^{5+} ions.

References

- [1] G.A.Smolensky, Physics of ferroelectric phenomena, Leningrad, Nauka, 1985 (in Russian).
- [2] G.A.Geguzina, A.T.Shuvaev, E.T.Shuvaeva, V.G.Vlasenko, Synthesis and structure of new phases of the $A_{m-1}\text{Bi}_2\text{B}_m\text{O}_{3m+3}$ ($m = 2$) type, *Cristallograph. Rep.*, **50**(2005), 59–64.
- [3] V.A.Isupov, Crystal chemical aspects of the bismuth-containing layered compounds of the $A_{m-1}\text{Bi}_2\text{B}_m\text{O}_{3m+3}$ type, *Ferroelectrics*, **189**(1996), 211–227.
- [4] L.Goux, J.G.Lisoni et al., Composition control and ferroelectric properties of sidewalls in integrated threedimensional $\text{SrBi}_2\text{Ta}_2\text{O}_9$ -based ferroelectric capacitors, *J. Appl. Phys.*, **98**(2005), 054507.

- [5] H. Yan, H. Zhang, R. Uvic, M. J. Reece, J. Liu, Z. Shen, Z. Zhang, A lead-free high-curie-point ferroelectric ceramic, $\text{CaBi}_2\text{Nb}_2\text{O}_9$, *Adv. Mater.*, **17**(2005), 1261–1265.
- [6] R. Macquart, B. J. Kennedy, T. Kamiyama, F. Izumi, Structural phase transitions in the ferroelectric oxides $\text{Ba}_{1-x}\text{Pb}_x\text{Bi}_2\text{Nb}_2\text{O}_9$ ($x = 0.375, 0.625$), *J. Phys.-Condes. Matter.*, **16**(2004), 5443–5452.
- [7] V. V. Kharton, E. N. Naumovich, A. A. Yaremchenko, F. M. B. Marques, Research on the electrochemistry of oxygen ion conductors in the former Soviet Union, *J. Sol. St. Electrochem.*, **5**(2001) 160–187.
- [8] K. R. Kendall, C. Navas, J. K. Thomas, H.-C. Loye, Recent developments in perovskite-based oxide ion conductors, *Sol. St. Ion.*, **82**(1995), 215–223.
- [9] K. R. Kendall, C. Navas, J. K. Thomas, H.-C. Loye, Recent developments in oxide ion conductors: Aurivillius phases, *Chem. Mater.*, **8**(1996), 642–649.
- [10] B. J. Kennedy, Q. Zhou, Ismunandar, Y. Kubota, K. Kato, Cation disorder and phase transitions in the four-layer ferroelectric Aurivillius phases $\text{ABi}_4\text{Ti}_4\text{O}_{15}$ ($A = \text{Ca}, \text{Sr}, \text{Ba}, \text{Pb}$), *J. Sol. St. Chem.*, **181**(2008), 1377–1386.
- [11] R. Macquart, B. J. Kennedy, Y. Shimakawa, Cation disorder in the ferroelectric oxides $\text{ABi}_2\text{Ta}_2\text{O}_9$, $A = \text{Ca}, \text{Sr}, \text{Ba}$, *J. Sol. St. Chem.*, **160**(2001), 174–177.
- [12] C. H. Hervoches, P. Lightfoot, Cation disorder in three-layer Aurivillius phases: structural studies of $\text{Bi}_{2-x}\text{Sr}_{2+x}\text{Ti}_{1-x}\text{Nb}_{2+x}\text{O}_{12}$ ($0 < x < 0.8$) and $\text{Bi}_{4-x}\text{La}_x\text{Ti}_3\text{O}_{12}$ ($x = 1$ and 2). *J. Sol. St. Chem.*, **153**(2000), 66–73.
- [13] Ismunandar, B. A. Hunter, B. J. Kennedy, Cation disorder in the ferroelectric Aurivillius phase $\text{PbBi}_2\text{Nb}_2\text{O}_9$: an anomalous dispersion X-ray diffraction study, *Sol. St. Ion.*, **112**(1998), 281–289.
- [14] I. J. Kennedy, B. J. Kennedy, Gunawan, Marsongkohadi, Structure of $\text{ABi}_2\text{Nb}_2\text{O}_9$ ($A = \text{Sr}, \text{Ba}$): refinement of powder neutron diffraction data, *J. Sol. St. Chem.*, **126**(1996), 135–141.
- [15] B. Wachsmuth, E. Zschech et al., Structure model of Aurivillius compounds. An EXAFS study, *Phys. Stat. Sol.(a)*, **135**(1993), 59–71.
- [16] T.-C. Chen, C.-L. Thio, S. B. Desu, Impedance spectroscopy of $\text{SrBi}_2\text{Ta}_2\text{O}_9$ and $\text{SrBi}_2\text{Nb}_2\text{O}_9$ ceramics correlation with fatigue behavior, *J. Mater. Res.*, **12**(1997), 2628–2637.
- [17] Y. Shi, Y. Pu, Q. Zhang, J. Li, L. Guo, Dielectric and multiferroic properties of two-layered $\text{SrBi}_2\text{Nb}_{2-x}\text{Fe}_x\text{O}_9$ Aurivillius compounds, *Ceram. Int.*, **44**(2018), S61–S64.
DOI: 10.1016/j.ceramint.2018.08.251
- [18] N. A. Zhuk, N. V. Chezhina, V. A. Belyy, B. A. Makeev, M. V. Yermolina, A. S. Miroshnichenko, Magnetic susceptibility of solid solutions $\text{Bi}_2\text{SrNb}_{2-2x}\text{Fe}_{2x}\text{O}_{9-\delta}$, *J. Magn. Magn. Mater.*, **451**(2018), 96–101. DOI: 10.1016/j.jmmm.2017.11.003
- [19] N. A. Zhuk, N. V. Chezhina et al., Influence of barium and strontium atoms on magnetic properties of iron-containing solid solutions $\text{Bi}_2\text{MNb}_2\text{O}_9$ ($M = \text{Ba}, \text{Sr}$), *J. Magn. Magn. Mater.*, **469**(2019), 574–579. DOI: 10.1016/j.jmmm.2018.09.027

- [20] N.A.Zhuk, N.V.Chezina, V.A.Belyy, B.A.Makeev, L.V.Rychkova, Magnetic behavior of $\text{Bi}_5\text{Nb}_{3-3x}\text{Fe}_{3x}\text{O}_{15-\delta}$ solid solutions., *Letters on Materials*, **7**(2017), 402–406.
DOI: 10.22226/2410-3535-2017-4-402-406
- [21] N.V.Chezina, D.A.Korolev et al., Structure, magnetic, and electrical properties of bismuth niobates doped with d-elements: XIV. Magnetic behavior of $\text{Bi}_2\text{BaNb}_{2-2x}\text{Fe}_{2x}\text{O}_{9-\delta}$ solid solutions, *Russ. J. General Chem*, **87**(2017), 168–174. DOI: 10.1134/S1070363217020037
- [22] N.V.Chezina, D.A.Korolev et al., Structure, magnetic, and electrical properties of bismuth niobates doped with d-elements: XV. Exchange interactions and state of iron atoms in the $\text{Bi}_5\text{Nb}_{3-3x}\text{Fe}_{3x}\text{O}_{15-\delta}$ solid solutions, *Russ. J. General Chem.*, **87**(2017), 373–380.
DOI: 10.1134/S1070363217030021
- [23] N.A.Zhuk, V.P.Lutov, B.A.Makeev, N.V.Chezina, V.A.Belyy, S.V.Nekipelov, ESR, NEXAFs study and magnetic properties of Fe-doped ferroelectric ceramics, *Rev. Adv.Mater. Sci*, **57**(2018), 35–41. DOI: 10.1515/rams-2018-0045
- [24] L.G.Akselrud, Yu.N.Grin, P.Yu.Zavaliy, V.K.Pecharski, V.S.Fundamentalski, CSD, an universal program package for single crystal and/or powder structure data treatment, Twelfth European Crystallogr. Meeting, Collected Abstracts, Moscow, 1989.
- [25] D.Y.Suarez, Relation between tolerance factor and T_{cin} Aurivillius compounds, *J. Mater. Res.*, **16**(2001), 3139–3149.
- [26] C.M.Wang, Electromechanical properties of A-site (LiCe)-modified sodium bismuth titanate ($\text{Na}_{0.5}\text{Bi}_{4.5}\text{Ti}_4\text{O}_{15}$) piezoelectric ceramics at elevated temperature, *J. Appl. Phys.*, **105**(2009) 463–467.
- [27] R.D.Shannon, Revised effective ionic radii and systematic studies of interatomic distances in halides and chalcogenides, *Acta Crystallogr.*, **A32**(1976), 751–767.
- [28] R.E.Vandenberghe, E.De Grave, Application of Mössbauer Spectroscopy in Earth Sciences, Mössbauer Spectroscopy. Tutorial Book, 2013, 91–185.
- [29] N.A.Lomanova, S.G.Semenov, V.V.Panchuk, V.V.Gusarov, Structural changes in the homologous series of the Aurivillius phases $\text{Bi}_{n+1}\text{Fe}_{n-3}\text{Ti}_3\text{O}_{3n+3}$, *J. Alloys Comp.*, **528**(2012), 103–108.
- [30] C.K.Matsuda, R.Barco, P.Sharma, V.Biondo, A.Paesano, J.B.M. da Cunha, B.Hallouche, Iron-containing pyrochlores: structural and magnetic characterization, *Hyperfine Interaction.*, **175**(2007), 55–61.
- [31] G.Filoti, M.Rosenberg, V.Kuncser, B.Seling, T.Fries, A.Spies, S.KemmlerSack, Magnetic properties and cation distribution in iron containing pyrochlores, *J. Alloys Comp.*, **268**(1998), 16–21.
- [32] N.A.Zhuk, V.P.Lutov et al., ESR and NEXAFS spectroscopy of $\text{BiNb}_{1-x}\text{Fe}_x\text{O}_{4-\delta}$ ceramics, *Physica B: Condensed Matter.*, **552**(2018), 142–146.
DOI: 10.17516/1997-1397-2018-11-5-615-621

- [33] N.A.Zhuk, M.V.Yermolina, V.P.Lutoev, B.A.Makeev, E.A.Belyaeva, N.V.Chezina, Phase transitions and magnetic properties of $\text{BiNb}_{1-x}\text{Fe}_x\text{O}_{4-\delta}$, *Ceram. Intern.*, **43**(2017), 16919–16923. DOI: 10.1016/ceramint.2017.09.094

ЭПР и ^{57}Fe -мёссбауэровская спектроскопия $\text{SrBi}_2\text{Nb}_2\text{O}_9$ допированного железом

Владимир П. Лютоев

Андрей Ю. Лысюк

ИГ ФИЦ Коми НЦ УрО РАН
Сыктывкар, Российская Федерация

Лариса О. Карлова

ОАО "Коми тепловая компания"
Сыктывкар, Российская Федерация

Дмитрий С. Безносиков

ФГУП "Главный радиочастотный центр", Филиал по Северо-Западному федеральному округу
Сыктывкар, Российская Федерация

Надежда А. Жук

Сыктывкарский государственный университет им. Питирима Сорокина
Сыктывкар, Российская Федерация

Аннотация. Твердофазным методом синтеза получены твердые растворы $\text{Bi}_2\text{SrNb}_{2-2x}\text{Fe}_{2x}\text{O}_{9-\delta}$. Методами ЭПР и мёссбауэровской спектроскопии исследовано электронное состояние и характер локального окружения атомов железа в матрице $\text{SrBi}_2\text{Nb}_2\text{O}_9$ со слоистой перовскитоподобной структурой. В спектрах ЭПР образцов твердых растворов $\text{Bi}_2\text{SrNb}_{2-2x}\text{Fe}_{2x}\text{O}_{9-\delta}$ ($x \leq 0.04$) присутствует интенсивная асимметричная линия в области низких полей с главной особенностью при $g = 4.27$, слабо выраженными пиком $g = 6.15$ и плечом $g \sim 9$, а также интенсивная широкая ($\Delta B_{pp} \sim 50\text{--}150$ мТ) полоса с центром около $g \sim 2.0$. Мёссбауэровский спектр соединения $\text{Bi}_2\text{SrNb}_{2-2x}\text{Fe}_{2x}\text{O}_{9-\delta}$ представлен асимметричным дублетом с изомерным сдвигом (IS) ~ 0.3 и квадрупольным расщеплением (QS) ~ 0.5 мм/с. Форма дублета воспроизводится суперпозицией двух дублетов с малыми и высокими значениями IS и QS. Около 85 % спектральной площади парамагнитной части спектра приходится на дублет $\text{Fe}^{3+}(1)$ with $\text{IS} = 0.31 \pm 0.04$, $\text{QS} = 0.45 \pm 0.04$ мм/с, соотношенный с ионами Fe^{3+} в регулярных аксиальных позициях. Оставшаяся часть представлена дублетом $\text{Fe}^{3+}(2)$ с $\text{IS} = 0.5 \pm 0.1$, $\text{QS} = 0.7 \pm 0.2$ мм/с от ионов Fe^{3+} в дефектном окружении.

Ключевые слова: фазы Ауривиллиуса, железо, ЭПР, мёссбауэровская спектроскопия.